

Unequal Code-Length Code Structure for Better Acquisition Performance in Weak Signal Environment

Zhang Xiang-li^{1,2}, Hu Xiu-lin, and Tang Zu-ping

¹ Huazhong University of Science and Technology, Wuhan 430074, China;

² China University of Geosciences, Wuhan 430074, China

Email: zhangxlcug@gmail.com; xlhu@mail.hust.edu.cn; tang_zuping@mail.hust.edu.cn

Abstract—In this paper, a new PRN code optimal design based on unequal-length code modulation is proposed. The better performance of code acquisition in weak signals will be achieved by using this method, because the cross-correlations between different signals have been sliding, thus suppressing multiple access interference effectively. Theoretical analysis and simulation show that this design has predictive power for compressing multi-access interference. Meanwhile, it does not need extra acquisition effort, thus it is convenient, feasible and effective.

Index Terms—GNSS, acquisition performance, weak signal environment, PN code

I. INTRODUCTION

The Global Navigation Satellite System (GNSS) is a satellite-based utility which provides users with accurate navigation and timing services worldwide. GNSS utilizes triangulation principle to determine the user position and timing information. PRN Codes are used by GNSS not only to spread the spectrum of the transmitted signal but also to allow retrieving ranging information. These codes look like and have spectral properties similar to random binary sequences but are actually deterministic.

The conventional PRN codes (such as GPS L1C/A) have a cross-correlation distance of 21.1 dB at worst-case Doppler difference. The distance is sufficient in nominal conditions. However, the requirements of location based and emergency caller localization services spurred by the E-911 mandate (USA) and the E-112 initiative (EU) have generated the demand for the availability of GNSS in weak signal environments[1]-[3]. A typical weak signal environment refers to the situation where powers of some visible satellite signals are obviously below the normal level. When the desired signal is weak and thus the detection threshold is set low, the presence of strong multi-access interference signals may lead to false alarms, because the cross-correlation peaks will be acquired as the autocorrelation peak. This problem is the result of the random time transmission delays between signals, which make it impossible to design the PRN codes assigned to each satellite to be completely orthogonal.

Various cross correlation mitigation techniques are used to deal with this problem [4-7]. The usual approach is to use longer codes to achieve extra protection against the strong cross-correlation, such as L2CM or L2CL. 3/14/2013 Although longer codes have some inherent advantages such as more diffuse line spectrum and the reduced vulnerability to CW interference, the search space and the computational complexity for signal acquisition become huge [8].

A technique for avoiding long pilot codes, Unequal Code Length Code Division Multiple Access (UCL-CDMA), was proposed in [9]-[10]. It was shown that good cross-correlation performance can be achieved with codes only a few hundred elements long if their lengths differ from each other. It can be regarded as a good compromise between the cross-correlation performance and computational complexity. Some theoretical analysis and practical methods for UCL-CDMA were described by previous literatures, but no detail analysis in frequency domain was put forward, neither assessments of performance were conveyed.

Based on the previous research, our work is presented as follows: we will begin, in Section II, by recalling the acquisition process in a GNSS receiver and presents the problem formulation in weak signal environment. In Section III, the principle and the design method of Unequal Code Length Code (UCLC) are introduced. This is followed in Section IV by assessing the performance of UCLC. Comparisons between the UCLC code and equal-length PN codes are also provided in this section. The cross-correlation, the decision probabilities and the mean acquisition time are considered as the measures. In Section V, results from simulated will be shown implementing the superior of UCLC. These simulations include post-correlation signal-to-noise-and-interference-radio (SNIR) and acquiring performance in different conditions. Finally, the conclusion is followed.

II. PROBLEM FORMULATION

A. Conventional Acquisition Process

The signal acquisition process is the first stage in the signal processing chain of a GNSS receiver. To perform signal acquisition, the receiver down-converts the Radio Frequency (RF) signals into an Intermediate Frequency (IF) signal. Then the digitized and sampled IF signal is passed to the acquisition module. The acquisition module generates the replica PN code of the desired satellite and

Manuscript received February 5, 2013; revised February 18, 2013, accepted March 6, 2013.

Corresponding author email: zhangxlcug@gmail.com

This work was supported by the Foundation Name under Grant No. 20110142120076

doi:10.12720/jcm.8.3.184-191.

correlates it with the IF received signal at all possible code delays and Doppler offsets. This process can be depicted as Fig. 1^[11]. It's a two-dimensional search in time (code phase) and frequency.

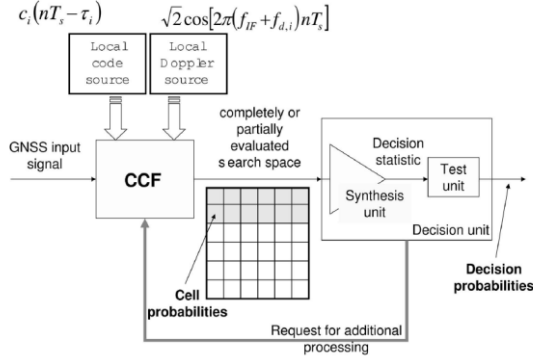


Figure 1. Schematic illustration of acquisition process

The time dimension is associated with the replica code, the frequency dimension is associated with the replica carrier. The combination of one code bin (code phase search increment) and one Doppler bin (frequency search increment) is called a cell. The set of all cells forms a matrix called the search space. The search space is swept until a “hit” (the test statistic is above the preset threshold) is found. Then the system goes to a verification phase that may include both an extended dwell time and an entry into a code tracking loop. Otherwise another pair of code phase and Doppler hypotheses is proposed and the acquisition process is repeated.

B. Problem Formulation In Weak Signal Environment

It is assumed that the received signal is composed of a desired signal plus a finite number of interfering signals and an additive noise $n(t)$. Within the receiver processing bandwidth, $n(t)$ has constant power spectral density. If the sampling rate of ADC is high enough, the digitized and sampled IF signal $r(t)$ can still be expressed by continuous function of time:

$$r(t) = \sum_{i=0}^K \left\{ \begin{array}{l} \sqrt{2C_i} d_i(t - t_{i,0}) c_i(t - t_{i,0}) \cdot \\ \cos(2\pi(f_{D_i} + f_i)t + \theta_i) + n(t) \end{array} \right\} \quad (1)$$

Signal with index 0 represents the desired signal. K is the number of all visible navigation signals except the desired one. Denote the i -th received signal power by C_i . Denote the power spectral density of the noise by N_0 . This IF signal $r(t)$ will correlate with the replica PN code and carrier (plus Doppler). Provided the pre-detection integration time is T_p , the correlation process can be expressed as:

$$v(t) = \frac{1}{T_p} \int_{(m-1)T_p}^{mT_p} r(t) c_0(t - \hat{t}_0) \sqrt{2} e^{2j\pi(f_i + \hat{f}_D)t + j\hat{\phi}_0} dt \quad (2)$$

where in \hat{t}_0 is the receiver's best estimate of code delay, \hat{f}_D is the receiver's best estimates of Doppler, and $\hat{\phi}_0$ is

the receiver's best estimates of carrier phase. m is the serial number of integration period.

Modernized GNSS signals are always composed of data and pilot (data-less) channels. The use of the pilot channel will extend applications to more challenging environments. And it can also provide increased reliability in the results. But the transmitted power is shared between two channels. The classical structure used to detect the useful signal using only one channel, thus after correlation with the replica PN code and carrier (plus Doppler), the I and Q values can be approximated by [12]:

$$I(t) = \sum_{i=0}^K \sqrt{\frac{C_i}{4}} d_i R_{0i}(\tau_i') \text{sinc}(\pi \hat{f}_{di} T_p) \cos(\phi_i') + n_I(t) \quad (3)$$

$$Q(t) = \sum_{i=0}^K \sqrt{\frac{C_i}{4}} d_i R_{0i}(\tau_i') \text{sinc}(\pi \hat{f}_{di} T_p) \sin(\phi_i') + n_Q(t) \quad (4)$$

τ_i' is the code delay error ($\tau_i' = t_{i,0} - \hat{t}_0$), ϕ_i' is the carrier phase delay error, \hat{f}_{di} is the frequency (Doppler) error $\hat{f}_{di} = f_{Di} - \hat{f}_D$. n_I and n_Q are independent Gaussian noises with equal power. $R_{0i}(\tau_i')$ is the cross correlation between the reference code and received code.

The conventional correlation seeks only the desired signal for detection and tracking, and the non-zero cross-correlation caused multi-access interference (MAI) would be zero if the PRN codes are designed to be perfectly orthogonal for random time delay τ_i' . Unfortunately, it is hardly possible to achieve this ideal result for the satellite-receiver asynchronous links and therefore MAI always exists. Hence, if the direct path undergoes large attenuations, the receiver could try to lock on the high cross correlation peaks in the presence of strong MAI. This represents a typical false acquisition case. It becomes worse as the number of interferers increases. Therefore, if the cross-correlation of PN codes can be reduced in weak signal reception environment, the acquisition performance of the desired signals can be improved effectively.

III. PRINCIPLE AND DESIGN METHOD OF UCLC

A. The Principle of UCLC

Using longer codes will reduce the PN code cross-correlation effectively, however the acquisition time and receiver complexity are rising as the code length increasing. In weak signal environment, the desired signal received power is lower than its nominal level 20 dB or more, which leads to a longer integration time and an increased computational load in the receiver. In order to keep the load within reasonable limits, it is desirable to limit the size of signal search space by using relatively short codes.

UCLC is a family of short codes to solve the problems limiting the current GNSS performances. The lengths of each PN code in the same family are co-prime to each other. Owing to the difference of code lengths, the cross-correlation between two UCLC codes varies in different

period of coherent integration while their autocorrelation keeping same. As coherent integration time extending, the auto correlation will be accumulated constantly, but cross correlation will not be accumulated in the same way. Therefore the cross-correlation performance can be improved obviously by using UCLC code. Fig. 2 shows a schematic illustration of the UCLC performance.

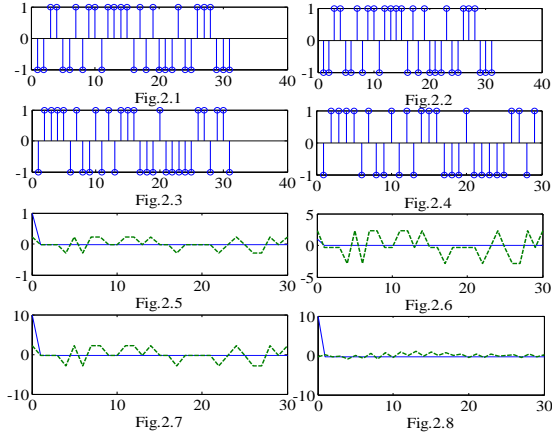


Figure 2. Schematic illustration of UCLC

In order to show the effects of UCLC more clearly, very short codes are used in the simulation. It's assumed that the PN code of the desired signal is 31-length balance GOLD sequence (Fig. 2.1, 2.2), one of the interfering signals adapts another equal-length GOLD sequence (Fig. 2.3) and the other adapts a truncated GOLD sequence (Fig. 2.4) of 29-length.

For $T_p = 1\text{ms}$, Fig. 2.5 shows the cross correlation between the equal-length codes and Fig. 2.6 shows that of un-equal length codes. In both figures, the blue line indicates the auto-correlation, the green line indicates the cross correlation. According to these figures, the cross-correlation properties of Gold sequences within 1ms are significantly better than that of the UCLC codes. However, for $T_p = 10\text{ms}$, the cross-correlation peaks of UCLC are obviously below that of equal-length codes. Fig. 2.7 shows that both the autocorrelation and cross-correlation peak of equal-length codes increase 10 times as coherent integration time expanding to 10ms. But the cross-correlation between UCLC codes not increase the same times as shown in Fig. 2.8. The cross-correlation performances of UCLC improve a lot as the coherent integration time extending. As a result, the acquisition performance improves accordingly.

The improvement of acquisition performance can also be explained in the frequency domain. Spectral separation coefficient (SSC) is commonly used in frequency domain analysis to characterize the influence of interference signals. Denote the normalized (unit area over emission bandwidth) signal's power spectrum by $G_s(f)$. Denote the normalized the interference's power spectrum by $G_I(f)$. And B represents the front-end filter bandwidth of GNSS receiver. The spectral separation coefficient (SSC)[13] is defined as:

$$\kappa_s = \eta^{-1} \int_{-B/2}^{B/2} G_I(f + \hat{f}_{dl}) G_s(f) df \quad (5)$$

When the data-less pilot channel is modulated by short code, its power spectrum will show line spectrum characteristics since the periodicity of the code. By using UCLC, the power spectrums of the desired signal and interfering signal will be staggered since the code lengths are co-prime to each other.

It can also be illustrated by simulation, as shown in Fig. 3. Provided that the desired signal is modulated by length-31 GOLD code, and the interference signal is modulated by length-29 truncated GOLD sequence. In Fig. 3, the red lines represent the desired signal line spectrum with line spacing of $1/31T_c$, and the blue lines represent the interference line spectrum with line spacing of $1/29T_c$. As the code length co-prime to each other, the two spectral lines are staggered completely.

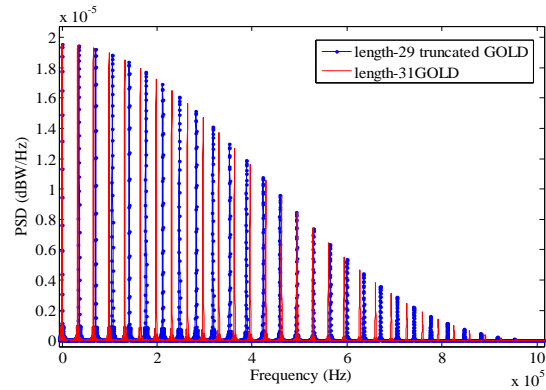


Figure 3. Two spectral lines staggered completely

Having recognized the effect of UCLC onto the signal PSD in the example above, now we want to see the transportation of this effect into the behavior of the spectral separation coefficient (SSC).

The SSC/Doppler characteristics have been simulated with an arbitrary access GPSL1 C/A signal as the desired signal, and another arbitrary access satellite as the interferer. For comparison purpose, the SSC/Doppler characteristics have also been simulated with two signals modulated by arbitrary access UCLC codes and random codes.

It is clear from the Fig. 4 that the SSC/Doppler characteristics of signals using equal-length code fluctuate very quickly for relative Doppler offsets equal to m -kHz where m is an integer (symbolized by the blue curve). But these fluctuations are little in most cases when using UCLC codes. And the SSC/Doppler characteristics of UCLC codes are almost identical to the spectral separation coefficient simulated with random codes (symbolized by the red curve).

The analysis of SSC provides a useful way to estimating the acquisition performance. For the assessment of acquisition performance, a metric commonly employed is the so called post-correlation SNIR. It is expressed as:

$$\rho_n = \frac{C_s \eta}{(N_0 + N_{0\text{eff}}) \cdot \frac{1}{T_p}} = \frac{T_p C_s \left[\int_{-B/2}^{B/2} G_s(f) df \right]}{N_0 + \sum_{l=1}^K C_l \kappa_{ls}} \quad (5)$$

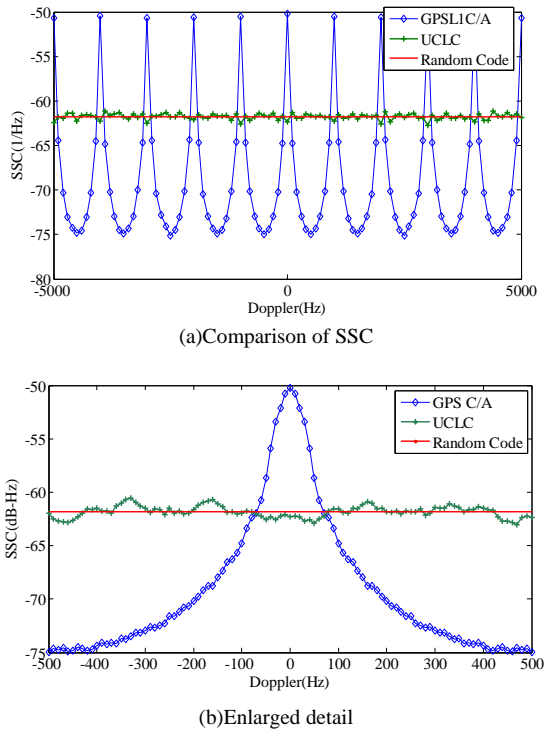


Figure 4. Comparison of SSC/Doppler characteristics

If SSC decreased, the SNIR will increase corresponding, and so the acquisition performance will be better. In weak signal environment, the interference dominates the noise. Thus, the ratio of the output SNIR can be simplified to the ratio of spectral separation coefficients, provided the powers of interference signals are same,

$$\frac{\rho'_n}{\rho_n} = \frac{N_0 + \sum_{l=1}^K C_l \kappa_{l_s}}{N_0 + \sum_{l=1}^K C_l \kappa'_{l_s}} \approx \frac{\sum_{l=1}^K C_l \kappa_{l_s \max}}{\sum_{l=1}^K C_l \kappa'_{l_s \max}} = \frac{\sum_{l=1}^K \kappa_{l_s \max}}{\sum_{l=1}^K \kappa'_{l_s \max}} \quad (6)$$

B. Design of UCLC

A block diagram that represents the modulation process of GNSS signals by different UCLC codes is shown in Fig. 5. Without loss of generality, provided that the first signal is the desired one and the others are interferences. If the desired signal is modulated by a L -length code, and the k -th interference is modulated by a $(L + \Delta k)$ -length code. Wherein Δk is an integer and $\Delta k \neq 0$, and $\gcd(L, L + \Delta k) = 1$. For the i -th signal and j -th signal, if $i \neq j$, then $\Delta i \neq \Delta j$.

Considering the number of satellites in a GNSS is 37[14]. A family of 37 UCLC codes can be generated as follow: taking 1023 as the reference code length to minimum the hardware modifications of the receiver. Then the lengths of UCLC codes should be as close as possible to 1023 to limit the size of signal search space by using relatively short codes. It's further required that the shortest and longest code length should differ as little as possible. A computer search for pair-wise prime numbers resulted in 37 integers.

Using the 37 integers as code lengths, a code search process is performed with a MATLAB program. It is also required that the codes be balanced. During the modulation process of GNSS signals, the chipping rate should keep same as the GPS C/A code in order to avoid timing confusion.

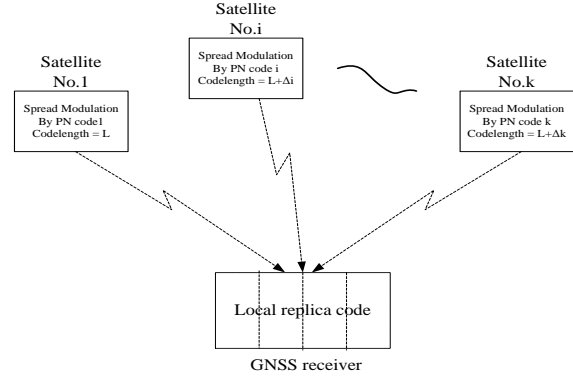


Figure 5. Schematic illustration of acquisition process

IV. PERFORMANCE OF UCLC EVALUATION

A. Cross-correlation Performance

Cross-correlation performance is one of the most important properties of the PN code family. The C/A code can offer 23.94 dB of cross-correlation protection at maximum capability. The L2 CM codes extend this figure to 28 dB. However, to achieve this cross-correlation performance requires the coherent signal observation period to be 20 ms for CM codes as opposed to 1 millisecond for C/A codes. This translates to increased acquisition effort, which naturally leads to the introduction of UCLC.

To verify the cross-correlation performance of UCLC, the codes generated in section III are used to calculate the worst cross-correlation as shown in Fig. 6. The cross-correlation values of L1C/A and L2C codes are also shown in Fig. 6 as the comparison. Each group of the performance curves in Fig. 6 represents the result of worst cross-correlation between corresponding 'raw' codes of UCLC, L1C/A and L2C. The horizontal axis of the figure represents the delay of codes in chips, while the vertical axis gives the cross-correlation value in dB.

The C/A code is a special case here as it belongs to the "Gold Code" family having controlled values of cross-correlation and therefore it has a flat response to all satellite combinations. On the other hand, a mean value of approximately 28 dB is also quoted as the cross-correlation protection figure for the CM code such as given in [15]. For the UCLC code, the variation of individual worst cross-correlations is limited by the integration time.

When the coherent integration time is only 1 ms, the cross-correlation performance of UCLC is definitely worse than L1C/A, as the blue triangles shown in Fig. 6. However when the coherent integration time is extended to 10ms, the cross-correlation performance of UCLC is better than L1C/A obviously, as the red stars shown in Fig. 6.

Further extending the integration time to 20ms(as long as that of L2CM), a much better cross-correlation protection will be achieved by UCLC, as the green stars shown in the figure.

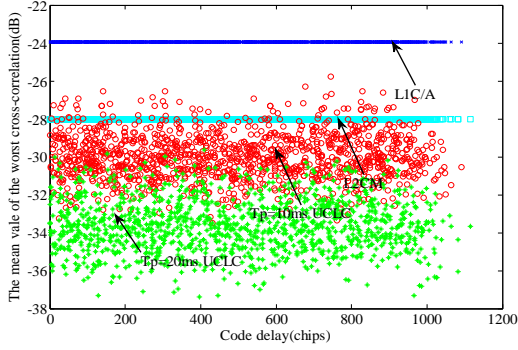


Figure 6. The worst correlations of L1C/A, L2M, and UCLC

Consequently, as a performance curve of UCLC moves towards the below, it indicates an improvement in the cross-correlation performance. This method of evaluating the cross-correlation performance is also used in [6]. The term ‘raw’ code refers to code sequences as they appear at the output of the corresponding code generator with 0s replaced by -1s and considering zero relative Doppler offset. The UCLC offers superior cross-correlation performance than L1C/A and requires less acquisition effort than the L2CM. Actually, when the coherent integration time is 20ms, the worst cross-correlation of UCLC is only -29.64dB while that of L2 CM is -25.39 dB (quaister2010), and L1C / A is -23.94dB. Therefore UCLC code can be the preferred choice for GNSS working in weak signal environments.

B. Probability of Detection

The acquisition performance of GNSS signal is always degraded by interferences especially in weak signal environment. However, difference in signal PN code modulation implies difference in protection against these interferences. Detection probability is one of key critical criterions of acquisition performance. In this section, detection probabilities are computed and compared for GNSS signals are modulated by L1C/A, UCLC, and L2CM.

The signal detection problem is based on a hypothesis test. Hypothesis H0: the useful signal is not present and H1: it is present.

Hypothesis H0: the useful signal is not present

The test statistic takes two different forms. The first one assumes that in the absence of the useful signal, there is only white thermal noise whereas the second one assumes that there are minor cross-correlation peaks.

In weak signal environment, both long coherent integration time and a great amount of non-coherent integration operations will be required.

Non-coherent integration uses the outputs generated from coherent integrations to achieve additional SNR gain. Although non-coherent integration suffers from a squaring loss, it still increases the SNR. When considering only the white Gaussian noise, the test statistic can be written as ^[15]:

$$D_0 = \sum_M (n_i^2(k) + n_Q^2(k)) \quad (7)$$

M is the non-coherent integration number. $n_i(k)$ and $n_Q(k)$ can be regarded as the Gaussian distribution. $\frac{D_0}{\sigma_n^2}$ is a central χ^2 (chi square) distribution. $2M$ represents the degrees of freedom of the central χ^2 distribution.

Now, if a minor cross-correlation peak is taken into account, the test statistic becomes

$$D_{0,J} = \sum_{k=1}^M \left[\left(\sum_{i=1}^K \sqrt{\frac{C_i}{4}} d_i R_{0i}(\tau_i') \frac{\sin(\pi \hat{f}_{dt} T_p)}{\pi \hat{f}_{dt} T_p} \cos(\varphi_i') + n_i(k) \right)^2 + \left(\sum_{i=1}^K \sqrt{\frac{C_i}{4}} d_i R_{0i}(\tau_i') \frac{\sin(\pi \hat{f}_{dt} T_p)}{\pi \hat{f}_{dt} T_p} \sin(\varphi_i') + n_Q(k) \right)^2 \right] \quad (8)$$

$\frac{D_{0,J}}{\sigma_n^2}$ is a noncentral χ^2 distribution with $2M$ degrees of freedom, the non-centrality parameter is

$$\lambda_J = \sum_{i=1}^K \frac{M}{f_p} \cdot \frac{C_i}{N_0} \left(R_{0i}(\tau_i') \text{sinc}(\pi \hat{f}_{dt} T_p) \right)^2 \quad (9)$$

Hypothesis H1: the useful signal is present.

In the case of a useful signal with only white Gaussian noise being present, the test statistic is derived as follows.

$$D_1 = \sum_{k=1}^M \left[\left(\sqrt{\frac{C_0}{4}} \cdot D \cdot R(\varepsilon_r) \text{sinc}(\pi \varepsilon_r T_p) \cos(\varepsilon_\phi) + n_i(k) \right)^2 + \left(\sqrt{\frac{C_0}{4}} \cdot D \cdot R(\varepsilon_r) \text{sinc}(\pi \varepsilon_r T_p) \sin(\varepsilon_\phi) + n_Q(k) \right)^2 \right] \quad (10)$$

$\frac{D_1}{\sigma_n^2}$ is a noncentral χ^2 distribution with $2M$ degrees of freedom, the non-centrality parameter is

$$\lambda_J = \frac{M}{f_p} \cdot \frac{C_1}{N_0} \left(R(\varepsilon_r) \text{sinc}(\pi \varepsilon_r T_p) \right)^2 \quad (11)$$

But in weak signal environment, the cross-correlation peak should be taken into account, therefore the non-centrality parameter is

$$\lambda_J = \frac{M}{f_p} \cdot \frac{C_1}{N_0} \left(R(\varepsilon_r) \text{sinc}(\pi \varepsilon_r T_p) \right)^2 + \sum_{i=2}^K \frac{M}{f_p} \cdot \frac{C_i}{N_0} \left(R_{0i}(\tau_i') \text{sinc}(\pi \hat{f}_{dt} T_p) \right)^2 \quad (12)$$

For the purpose of comparison, the detection probabilities of different PRN code modulations are calculated under the same receiver conditions. Usually P_{fa} is given and the corresponding threshold is computed. And then detection probability is deduced.

Provided $P_{fa} = 10^{-3}$, the signal-to-noise power spectral density ratio C/N_0 is 45dB, the threshold can easily be deduced by inverting function according to the expressing as follow.

$$P_{fa} = \Pr[D_0 > Th] = \int_{Th}^{\infty} P_{D_0}(y) dy = f(Th) \quad (13)$$

In order to simplify the process of simulation, we assume one signal as desired signal and another signal as multiple access interference, the PN code of both signals are chosen arbitrarily. And since the worst cross-correlation plays a important role in weak signal environment, the assumption H0 and assumption H1 are both non-central χ^2 distribution, the non-centrality parameters are expressed as (8) and (11) respectively . The detection probability is plotted as the function of C/N_0 ranging from 20 dB/Hz to 40 dB/Hz in Fig. 7.

The three curves express the relationship with the non-coherent integration number $M=30$. In the figure, the effects of front-end are not considered and the uncertainties of code delay, carrier frequency, and carrier phase are assumed to be zero.

As shown in Fig. 7, the detection probability of UCLC is significantly higher than that of L2CM and L1C / A under the same reception conditions.

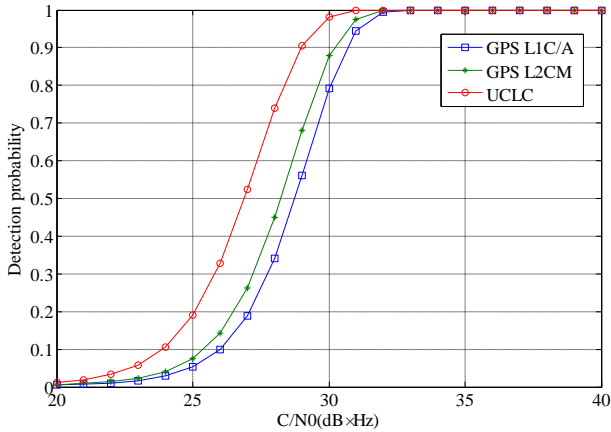


Figure 7. Average probabilities of detection with considered reference codes $P_{fa}=10^{-3}$, $M=30$, $T_p=20\text{ms}$

C. Mean Acquisition Time

Besides detection probability, mean acquisition time is another parameter used to measure the acquisition performance. It is the average time taken to acquire the signal over the given search space. The acquisition strategy studied here is the single dwell time search, and so the mean acquisition time is given as [Holmes, 1990]

$$\bar{T} = \left[\frac{2 + (2 - P_d)(q-1)(1 + K_p P_{fa})}{2P_d} \right] MT \quad (14)$$

where q is the entire uncertainty region to be searched, K_p is the penalty factor for time lost due to false alarms. M is the non-coherent integration number. The uncertainty region is dependent on the replica code design.

The search space is dependent on the replica code design, as given by

$$q = N_c \times N_d \quad (15)$$

where N_c is the number of code bins and N_d is the number of Doppler bins. For the purpose of comparison, the search dwell time of all three kinds of PN codes should be same. To improve the performance of weak signal acquisition, the single search dwell time is set long. Provided T is 20ms, the Doppler range is $[-9, +9] \text{ kHz}$, each Doppler bin is roughly $\frac{2}{3T} \text{ Hz}$, wherein T is the search dwell time. Thus the number of Doppler bins is 540.

Considering each code bin is typically $\frac{1}{2}$ chip, then the search space of GPS L1C / A code is 2046×540 cells, the search space of GPS L2CM code is 2046×540 cells. The search space of UCLC (the longest code length is 1151) is 2232×540 cells. With the same false alarm probability (P_{fa}) and probability of detection (P_d), the search space of UCLC is close to L1 C/A, far less than that of L2CM code.

On the other side, comparison of detection probability under same operating conditions is another useful way to estimate mean acquisition time of different PN codes. Provided $C/N_0 = 23 \text{ dB/Hz}$, the non-coherent number $M=30$, false alarm probability $P_{fa} = 10^{-3}$, detection probability of UCLC is 0.95, detection probability of L2CM is 0.64, detection probability of L1C/A is 0.48, as shown in Fig. 8. For a given K_p , substituting these figures of P_d into (13), it's obviously that UCLC showing good performance of the capture, and greatly reduce the acquisition time.

For a given K_p , substituting P_d into (15), it's obviously that the UCLC can be the preferred choice for satellite acquisition in GPS receivers working in weak signal environments.

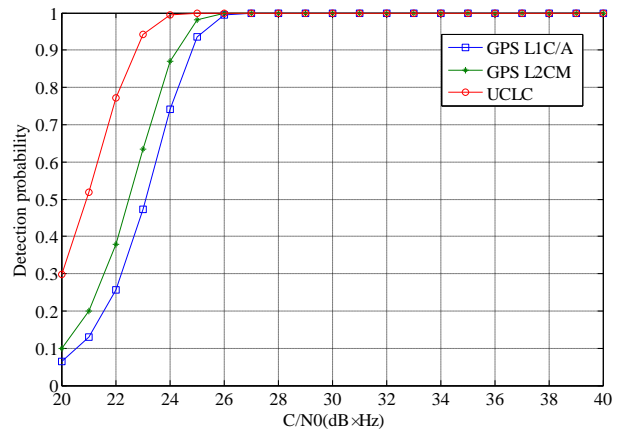


Figure 8. Comparison of detection probability under same operating conditions

V. SIMULATION RESULTS

UCLC may solve the near-far problem because there is an obvious improvement of cross-correlation. Therefore better acquisition performance can be achieved in weak signals environment. The advantage of the UCLC codes

is twofold: first, there's benefit in SNR to employing UCLC, and second, by using UCLC modulated signals, it's easier to identify the auto-correlation peak. To verify these two aspects, two cases of different scenarios are simulated:

Case 1 shows an example of satellite SNR improvements

Case 2 shows an example of satellite acquisition performance improvements.

Case 1: Here the simulated signal consists of four satellite signals and a strong multi-access interference. Provided the front-end bandwidth is 10MHz, the power spectral density of the noise $N_0 = -203\text{dB/Hz}$. All satellite signals was at low power levels with a pre-correlation SNR of -17 dB and the power of the interference signal was increased in steps of 10 dB from -3dB to 27dB SNR. For different coherent integration time, the post correlation SNRs are compared for the conventional L1C/A and UCLC codes as seen in Fig. 9.

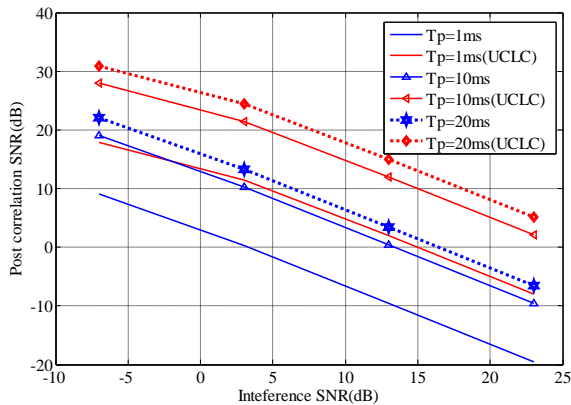


Figure 9. Improvement of Post-correlation SNR performance by UCLC

Case 2: Here again four satellite signals and one MAI signal. All parameter of simulation kept the same with case 1 except the power of the interference. The power of the interference signal was increased in steps of 10 dB from 10dB to 30dB above the desired signal. For different coherent integration time and different interference power, the acquisition performance are compared for the conventional L1C/A and UCLC codes. The strong interference signal prevents acquisition with the conventional L1C/A, but a good acquisition performance is achieved using UCLC as seen in figure 10.

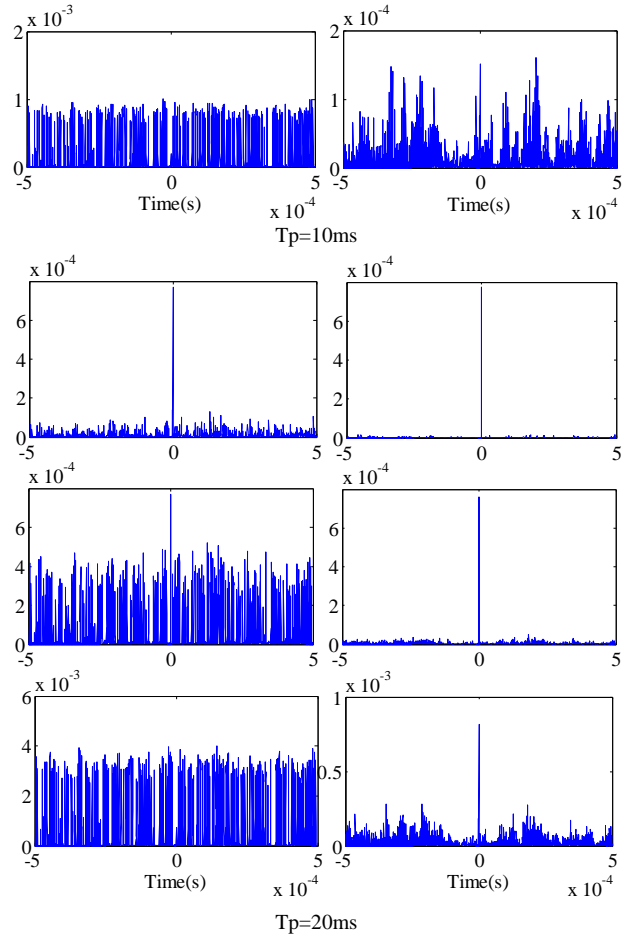
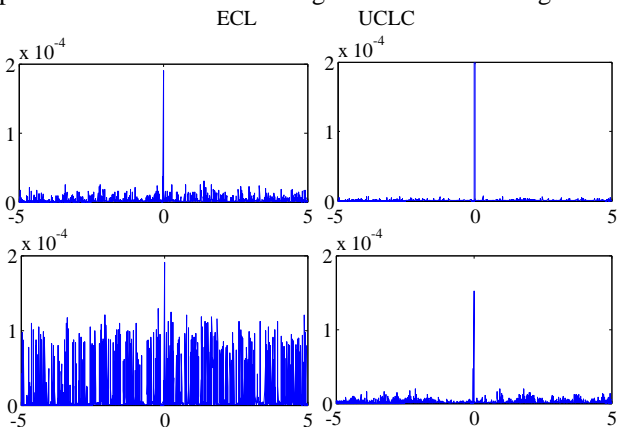


Figure 10. Improvement of acquisition performance by UCLC

VI. CONCLUSION

In this paper, a novel code structure for GNSS based on Unequal Code Length CDMA (UCL-CDMA) has been presented. The simulation results have shown that the family of short codes: UCLC has tremendous potential in making the GNSS receiver to achieve better acquisition performance in weak signal environment while the conventional short codes such as GPS L1C/A fail to detect the satellite signals at these levels. By the way, neither extra cost of hardware nor extra load is required in the GNSS receiver to achieve this performance.

The UCLC is shown to be a good method to cancel MAI, and at the same time to improve the acquisition performance in weak signal environment. We expect this design to be useful additions to modern designs of GNSS signal structure.

More research is needed to understand the effect of different pulse waveforms and data modulation on UCL-CDMA signals. The system level impact of unequal code lengths on data frame structure also requires further investigation.

REFERENCES

- [1] S. U. Qaisar and A. G. Dempster, "Cross-correlation performance assessment of global positioning system (GPS) L1 and L2 civil

codes for signal acquisition,” *IET Radar, Sonar and Navigation*, vol. 3, pp. 195–203, May 2011.

[2] T. H. Ta, S. U. Qaisar, A. G. Dempster, and F. DAVIS, “Partial differential postcorrelation processing for GPS L2C signal acquisition,” *IEEE Transactions on Aerospace and Electronic Systems*, vol. 48, pp. 1287-1305, April 2012.

[3] S. U. Qaisar and A. G. Dempster. “Assessment of the GPS L2C code structure for efficient signal acquisition,” *IEEE Transactions on Aerospace and Electronic Systems*, vol. 48, pp. 1889-1902, July 2012.

[4] P. Madhani, P. Axelrad, K. Krumvieda, and J. Thomas, “Application of interference cancellation to the GPS near-far problem,” *IEEE Transactions on Aerospace and Electronic Systems*, vol. 39, pp. 481-488, April 2003.

[5] E. P. Glennon and A. G. Dempster, “Delayed PIC for postcorrelation mitigation of continuous wave and multiple access interference in GPS receivers,” *IEEE Transactions on Aerospace and Electronic Systems*, vol. 47, pp. 2544-2557, October 2011.

[6] M. Miller, J. Tsui, D. Lin, and Q. H. Zhou, “GPS civil signal self-interference mitigation during weak signal acquisition,” *IEEE Transactions on Signal Processing*, vol. 55, pp. 5859-5863, December 2007.

[7] H. Z. Li and F. Zhao, “Multi-User Detection Technology of CDMA System,” in *Proc. International Conference on Electronics and Optoelectronics*, Dalian, China, 2011, v. 2, pp. 210-212.

[8] D. Borio, C. O. Driscoll, and G. Lachapelle, “Composite GNSS signal acquisition over multiple code periods,” *IEEE Transactions on Aerospace and Electronic Systems*, vol. 46, pp. 193-206, January 2010.

[9] Z. D. Q and T. Seppo, “Multiple access using different codes lengths for global navigation satellite systems,” U.S. Patent 7 298 780 B2, Nov 20, 2007.

[10] Q. Zhengdi and S. Turunen. “Nearly orthogonal codes in GNSS using unequal code lengths,” in *Proc. ION 60th Annual Meeting*, Dayton, Ohio, 2004, pp. 666-670.

[11] B. Daniele and C. Laura, “Impact of GPS acquisition strategy on decision probabilities,” *IEEE Transactions on Aerospace and Electronic Systems*, vol. 44, pp. 996-1011, July 2008.

[12] O. Julien, “Design of galileo 11f receiver tracking loops,” Ph.D. dissertation, Dept. Geomatics Eng, University of Calgary, Canada, July 2005.

[13] J. W. Betz and K. R. Kolodziejcki. “Generalized theory of code tracking with an early-late discriminator part I: Lower Bound and

Coherent processing,” *IEEE Transactions on Aerospace and Electronic Systems*, vol. 45, pp. 1539- 1550, Oct 2009.

[14] E. D. Kaplan and C. J. Hegarty, *Understanding GPS Principles and Applications*, 2nd ed, Artech House, 2006.

[15] S. U. Qaisar, “Receiver strategies for GPS L2C signal processing,” Ph.D. dissertation, School of Surveying & Spatial Information Systems. University of New South Wales, Australia, March 2010.



Zhang Xiang-li was born in Hebei, China, in 1977. She received her bachelor degree in Electrical Engineering (EE) in 1999 from Hebei university of science and technology, and her Master degree in communication and system in 2005 from Beihang University. Now she is an candidate of Ph.D in Huazhong university of science and technology, Wuhan, China. Her primary research interest is in the optimization design of PN codes and interference mitigation techniques in future navigation system.



Hu Xiu-lin was born in Henan, China. He is a professor of Huazhong university of science and technology. His major is communication system and aerospace engineering. His research interests are receiver development, research about future navigation system design, and interference mitigation techniques.



Tang Zu-ping was born in Chongqing, China, in 1981. He received his B.S. and M.S. degree in 2002 and 2005 and the Ph.D.degree in aerospace engineering in 2009, all from Huazhong university of science and technology His research interests are receiver development, research about future navigation system design, and interference mitigation techniques.